

Battery State-of-health Adaptive Energy Management of Hybrid Electric Vehicles

Original

Battery State-of-health Adaptive Energy Management of Hybrid Electric Vehicles / Anselma, Pier Giuseppe; Kollmeyer, Phillip; Emadi, Ali. - (2022), pp. 1035-1040. (2022 IEEE Transportation Electrification Conference & Expo (ITEC) Anaheim, CA, USA 15-17 June 2022) [10.1109/ITEC53557.2022.9813796].

Availability:

This version is available at: 11583/2969960 since: 2022-07-08T15:29:03Z

Publisher:

IEEE

Published

DOI:10.1109/ITEC53557.2022.9813796

Terms of use:

This article is made available under terms and conditions as specified in the corresponding bibliographic description in the repository

Publisher copyright

IEEE postprint/Author's Accepted Manuscript

©2022 IEEE. Personal use of this material is permitted. Permission from IEEE must be obtained for all other uses, in any current or future media, including reprinting/republishing this material for advertising or promotional purposes, creating new collecting works, for resale or lists, or reuse of any copyrighted component of this work in other works.

(Article begins on next page)

Battery State-of-health Adaptive Energy Management of Hybrid Electric Vehicles

Pier Giuseppe Anselma^{1,2}, Phillip Kollmeyer³, Ali Emadi³

¹Department of Mechanical and Aerospace Engineering (DIMEAS), Politecnico di Torino, Torino, Italy

²Center for Automotive Research and Sustainable Mobility (CARS), Politecnico di Torino, Torino, Italy

³McMaster Automotive Resource Center (MARC), McMaster University, Hamilton, ON, Canada

E-mail: pier.anselma@polito.it

Abstract- Effectively adapting the hybrid electric vehicle (HEV) powertrain operation as a function of the battery state-of-health (SOH) can lead to significant energy savings over the entire vehicle lifetime. This paper demonstrates the potential of a heuristic HEV energy management strategy (EMS) that is calibrated to adaptively minimize fuel consumption as the battery loses capacity due to ageing. A power-split HEV powertrain is used for this case study, and a heuristic EMS approach which does not adapt to battery ageing is used as the baseline. Particle swarm optimization (PSO) is implemented to tune the parameters of the baseline EMS to minimize fuel consumption. Then, the battery SOH adaptive HEV EMS is developed with parameters which are a function of battery SOH. The parameters are tuned with PSO as well. A battery SOH dependent model is created from experimental data from an ageing test which continued until SOH reached 16%. Simulation results demonstrate that the proposed battery SOH adaptive EMS achieves as much as 20% better fuel economy than the non-adaptive controller as the battery ages. An EMS for HEVs which controls the vehicle powertrain as a function of battery SOH is therefore critical to maintaining minimal fuel consumption throughout the life of the vehicle.

I. INTRODUCTION

Hybrid electric vehicles (HEVs) can achieve significantly less tailpipe emissions than conventional internal combustion engine (ICE) vehicles, and HEVs are conveniently not dependent on charging infrastructure like electric vehicles [1]. In HEVs, batteries are essential for storing energy as the second fundamental source of propulsion for the vehicle. The batteries power electric motor/generators (EMs) which allow the ICE to be used at more efficient points and to be shut off when unneeded. Furthermore, vehicle batteries allow the capture of regenerative braking energy, which would otherwise be dissipated as heat in the brakes [2]. HEV energy management strategies (EMSs) are necessary to control the flow of power through the system to minimize fuel consumption. As the vehicle batteries age though their capacity decreases and their resistance increases, reducing the energy and power available to support the hybrid powertrain [3][4]. This ageing must be considered in the EMS so that fuel consumption does not increase unnecessarily throughout the lifetime of the vehicle.

Multiple studies have investigated the impact of battery ageing on electrified vehicles. Herb et al. in 2013 modeled the performance decay of a fuel cell electric vehicle by considering battery power capability to be reducing linearly over time [5].

In 2015, Saxena et al. assessed how battery capacity fade and a decrease in power capability could affect the ability of battery electric vehicles to fulfill the users' daily travel requirements [6]. Last year Anselma et al., the authors of this paper, evaluated the reduction in fuel economy and worsening drivability of a full HEV as the battery aged down to 16% state-of-health (SOH) [7]. Experimental characterization data for a battery cell, including open-circuit voltage (OCV), resistance, charge and discharge power capabilities, were collected throughout the life of the cell. Then, the fuel economy capability was estimated by implementing an offline, optimal dynamic programming (DP) algorithm.

The prior research highlights how battery parameters vary throughout lifetime and their impact on the vehicle. Nevertheless, HEV EMSs presented in the literature are almost always developed and calibrated considering only a new battery, i.e. SOH of 100%. As a consequence, the fuel economy could significantly worsen due to battery ageing. However, not much research has been conducted for optimally adapting the parameters of the HEV EMS to preserve enhanced fuel economy as the battery ages. To answer this need, this paper proposes an online battery SOH adaptive EMS for HEVs. An optimization-based calibration of the EMS parameters is performed at various levels of battery SOH. Then, the obtained SOH adaptive controller is benchmarked against a non-adaptive version of the same HEV EMS throughout the battery lifetime.

The paper is structured as follows: the HEV numerical model and baseline EMS are illustrated first. Then, the development the SOH adaptive EMS and optimization-based EMS calibration are discussed. Simulation results throughout battery lifetime are presented, and finally conclusions are given.

II. HEV MODEL AND ENERGY MANAGEMENT STRATEGY

The HEV powertrain layout used is that of the third generation Toyota Prius® hybrid. This HEV powertrain represents a well-known layout from the state-of-the-art, and many related open-source data regarding it are available [8]. The battery is assumed to consist of LiFePO₄ cells tested by the authors [10], rather than the NiMH cells used in the Prius®. The HEV specifications considered here are reported in Table I and the hybrid powertrain is illustrated in Fig. 1.

TABLE I
ASSUMED HEV PARAMETERS

Component	Parameter	Value
Vehicle	Mass	1531 kg
	RL_A	90.0 N
	RL_B	0.20 N/(m/s)
	RL_C	0.42 N/(m/s) ²
ICE	Capacity	1.8 L
	Power max	72 kW @ 5,000 rpm
	Torque max	142 Nm @ 4,000 rpm
EM1	Power max	42 kW
EM2	Power max	65 kW
Transmission	PG ratio (Ring / Sun)	2.6
	Gear ratio (EM2)	1.26
	Differential ratio (i_{FD})	3.27
	Efficiency (EV mode)	0.95
	Efficiency (HEV mode)	0.85
Auxiliaries	Electrical subsystem power	500 W
Battery	Pack capacity	1.82 kWh
	Pack configuration	120S – 2P
	Cell type	A123 ANR26650M1-B

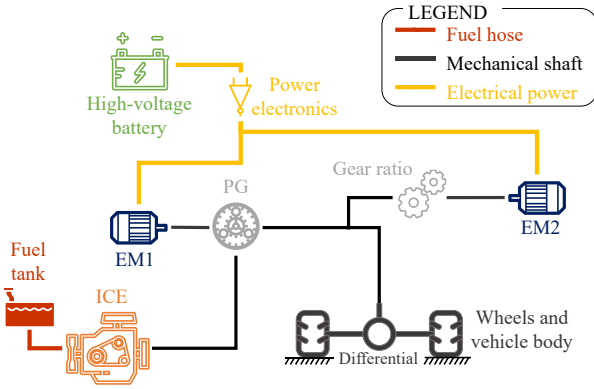


Fig. 1 Toyota Prius Gen3 hybrid powertrain layout.

A. HEV numerical model

The HEV powertrain is modeled here in Matlab® using a backward quasi-static approach for evaluating the requested power values and the speed of components directly from the driving mission requirements. Particularly, the driver's power demand, P_{wheels} , in watts can be determined following a road load modelling approach and using (1):

$$P_{wheels} = (RL_A + RL_B \cdot v_{veh} + RL_C \cdot v_{veh}^2 + m_{eq} \cdot a_{veh}) \cdot v_{veh} \quad (1)$$

Where RL_A , RL_B and RL_C are the vehicle road load coefficients. v_{veh} and a_{veh} stand for the vehicle speed and the vehicle acceleration, respectively, as provided at each time instant by the driving mission requirements.

As shown in Fig. 1, the EM2 angular speed directly depends on the angular speed of the differential input shaft. On the other hand, the planetary gear (PG) set allows the ICE speed to be decoupled from the vehicle speed. Thus, speed and torque of

the ICE can be controlled arbitrarily by the EMS, while the EM1 speed and torque are a function of both the vehicle speed and the controlled values of ICE speed and torque and following the planetary gear ratios. The interested reader can find more details in [9]. As concerns the transmission mechanical efficiency, different values are retained depending on pure electric (EV) or hybrid electric (HEV) operation in Table I. Particularly, lower efficiency is considered in HEV mode since the higher number of gear engagement points in the PG sets increases the overall transmission meshing losses.

Instantaneous fuel consumption as well as electrical loss of the EMS are evaluated by means of empirical lookup tables with torque and speed as independent variables. For the A123 battery cells, which are LiFePO₄ and rated for 2.5 Ah, an equivalent circuit model is adopted with open-circuit voltage, internal resistance, charge power capability, discharge power capability and residual capacity values which are dependent on the instantaneous values of both state-of-charge (SOC) and SOH. Experimental battery ageing results presented in [7] and in [10] are used to model the battery parameters as a function of ageing.

B. Baseline HEV EMS

The EMS used in this work is illustrated in Fig. 2 and it is based off the EMS for the production Toyota Prius HEV powertrain. It includes control of the ICE state, ICE power, and ICE speed and torque [11].

At each simulation time instant, the value of P_{wheels} is determined first. Then, the ICE state is set to on if either the battery SOC is below a given lower threshold SOC_{low} or the requested wheel power is above an upper threshold P_{up} which cannot be supplied by the battery pack alone. The ICE is kept on until either the battery SOC exceeds a given upper threshold SOC_{up} or the requested wheel power is lower than a certain threshold P_{low} . Different upper and lower threshold values are used to reduce the frequency of ICE activations. After the first cranking event in a drive cycle, the ICE is forced to keep running for a certain amount of time before being deactivated to warm up the catalytic converter. In this work, the ICE is kept activated for at least 90 seconds after it is first started since a stabilization in particulate emissions has been observed after this amount of time [12].

When the ICE is on, ICE power P_{ICE} is set to a value interpolated from a one-dimensional lookup table with battery SOC as the independent variable. In general, ICE power is set higher for lower battery SOC. The calibration of the ICE power lookup table throughout battery lifetime is the focus of the next section.

Any combination of ICE speed and torque which achieves P_{ICE} can be used due to the drivetrain's planetary gear configuration, as illustrated in Fig. 1. The ICE speed and torque are set to follow the optimal operating line (OOL), which is the combination of speed and torque that minimizes the fuel rate for each given value of ICE mechanical power. Once all the control variables are set (i.e. ICE on/off state, power, speed, and torque), speed and torque of the EMS and

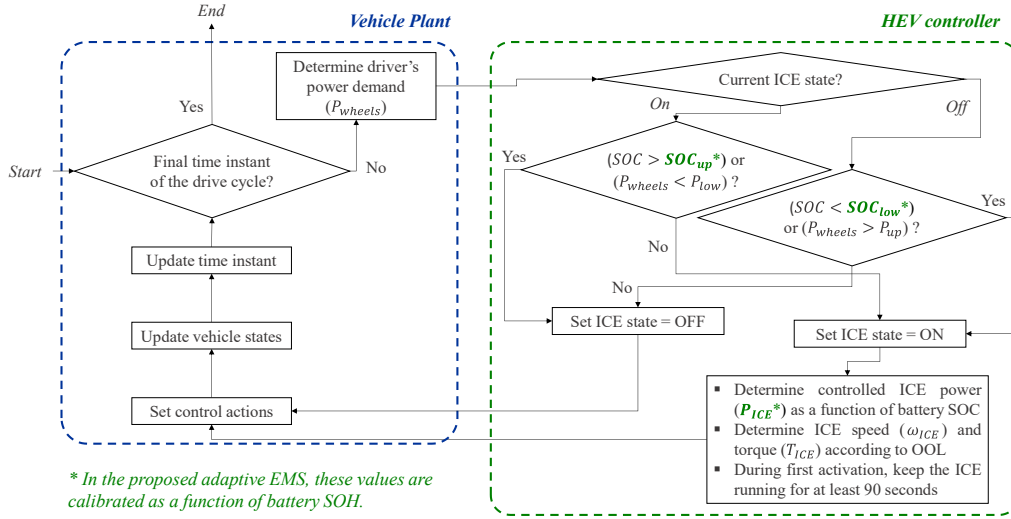


Fig. 2 Workflow of the HEV EMS.

the battery power can automatically be determined via a backward modelling approach.

Three further control rules are set here: 1) if the battery power exceeds the corresponding power capability, the ICE power is adjusted to meet the requested wheel power while complying with battery operational limits, 2) if the wheel power is negative (i.e. the vehicle is braking), the ICE is constrained to not deliver braking torque to improve the driving response of the vehicle, 3) if the vehicle is braking and the battery pack charge power capability is less than the braking power, friction brakes are set to provide the remaining share of braking power required. As consequence, when the vehicle is braking during HEV mode and the ICE is set to operate since the battery SOC is still lower than SOC_{up} , the ICE is kept in an idle state.

Once the controlled values of ICE speed and torque are determined by the EMS, the next step in Fig. 2 involves setting them in the HEV plant model. Then, the vehicle states (e.g. cumulative fuel consumption, battery SOC) are updated according to the numerical HEV plant model. Finally, the simulation time step is updated and the workflow is iterated in the following time instant of the drive cycle under analysis.

III. OPTIMIZATION-BASED CALIBRATION OF THE SOH ADAPTIVE HEV EMS

This section presents the calibration of the parameters for the heuristic HEV EMS presented in section 2. The implemented calibration workflow is illustrated in Fig. 3. Particle swarm optimization (PSO) algorithm is used here to calibrate the parameters of the HEV EMS [13]. For the baseline HEV EMS (i.e. non-battery SOH adaptive), 8 parameters require calibration: 1) SOC_{up} ; 2) SOC_{low} ; 3) 6 discretized values of P_{ICE} as a function of battery SOC. The values for P_{up} and P_{low} are selected based on battery power capability and drivability criteria and are kept constant for all the simulations. As shown in Fig. 3, the baseline HEV EMS is calibrated first using PSO by iteratively simulating the HEV performing the worldwide harmonized light vehicle test procedure (WLTP) with battery SOH equal to 95%. The parameters are calibrated to minimize equivalent fuel consumption, which is calculated to capture any net energy consumed from the battery. Then, the same workflow is repeated for the battery SOH adaptive HEV EMS. However, the process is more complicated and computationally expensive because: 1) the 8 calibration parameters are tuned for 4 different values of battery SOH (i.e. totally 32 parameters require calibration by PSO), 2) each

EMS calibration using PSO (Section III):

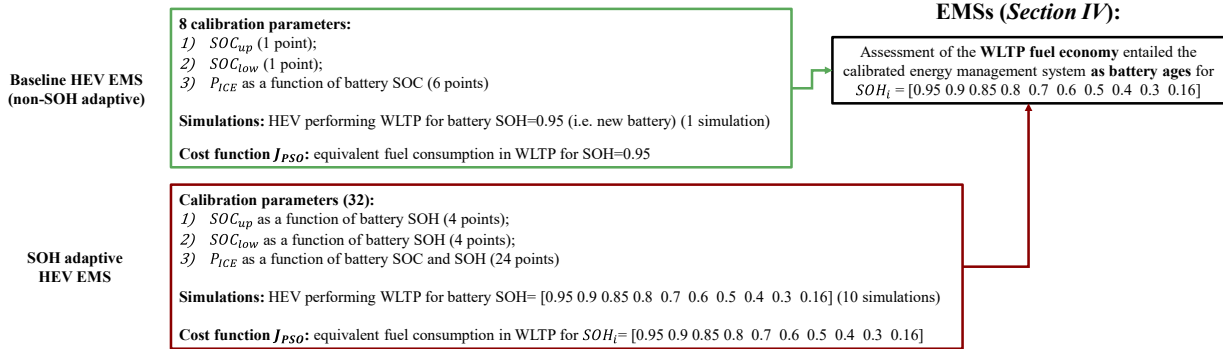


Fig. 3 Workflow for calibrating and assessing the baseline HEV EMS and the battery SOH adaptive HEV EMS.

option for the EMS parameter set is evaluated by simulating the HEV in WLTP not only with new battery conditions, but also with aged battery conditions: totally 10 different values of battery SOH are considered in this step (i.e. the total number of simulations increases by 10 times compared with the baseline workflow) to further improve the calibration accuracy without increasing the number of EMS parameters to be tuned, 3) the PSO calibration cost function involves minimizing the average HEV equivalent fuel consumption for the considered battery SOH values. The cost function J_{PSO} that PSO needs to minimize within the calibration process of the SOH adaptive HEV EMS can be expressed as follows:

$$J_{PSO} = -\frac{1}{\sum_{i=1}^N [M_{fuel-eq}(i) + \Delta_i]}$$

with

$$M_{fuel-eq_i} = Fuel_i + \frac{E_{batt}(i)}{LHV_{fuel} \cdot \bar{\eta}_{ICE} \cdot \text{sign}[E_{batt}(i)](i)}$$

$$\Delta_i = \begin{cases} 0 & \text{if } |E_{batt_i}| \leq 0.01 \cdot LHV_{fuel} \cdot Fuel_{cons}(i) \\ 1e6 & \text{if } |E_{batt_i}| > 0.01 \cdot LHV_{fuel} \cdot Fuel_{cons}(i) \end{cases} \quad (2)$$

$$Fuel_{cons}(i) = \int_{t_0}^{t_{end}} \dot{m}_{fuel}(\omega_{ICE}, T_{ICE}, t) dt$$

$$E_{batt}(i) = \int_{t_0}^{t_{end}} [OCV_{pack}(SOH_i, SOC, t) \cdot I_{pack}(P_{ICE}, SOH_i, SOC, t)] dt$$

where $M_{fuel-eq}(i)$ is the equivalent fuel consumption of the HEV in the i -th simulation among the N simulations performed by varying the value of battery SOH. Looking at Fig. 3 and following the description provided in this section, N equals to 10 in this work and considers values of battery SOH ranging from 0.95 down to 0.16. $M_{fuel-eq}$ can be evaluated by integrating the sum of two terms over time from the initial time instant of WLTP t_0 to the final one t_{end} . $Fuel(i)$ stands for the overall fuel consumption in the i -th simulation as obtained by integrating over time the instantaneous value of fuel rate \dot{m}_{fuel} which is obtained by interpolating in the empirical map with ICE speed and torque as independent variables. $E_{batt}(i)$ is the net battery energy variation in joules for the i -th simulation and it can be evaluated by integrating over time the product of the battery pack OCV and current. LHV_{fuel} is the fuel lower heating value, while $\bar{\eta}_{ICE}(i)$ is the average ICE efficiency in the i -th simulation. Δ_i is a weighting factor that aims at penalizing the set of calibrated values for the SOH adaptive EMS which do not lead the HEV to operate in charge-sustaining operation in the i -th simulation. This is performed to prevent the EMS to save fuel by excessively depleting the SOC of the battery pack, which would be undesirable in real-world operation. In this work, the procedure defined by the US Environmental Protection Agency (EPA) and endorsed by SAE J1711 is considered as criterion for determining HEV charge-sustaining operation. This process involves a net battery energy variation tolerance [14]. It should be reminded that the formulation of

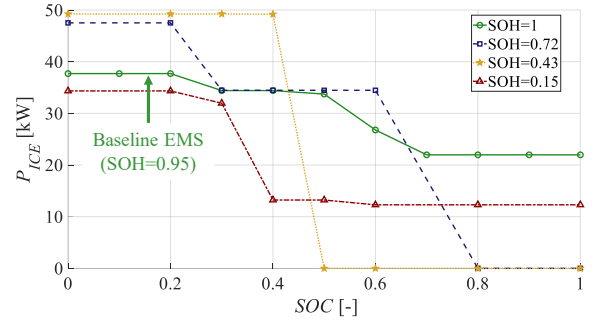


Fig. 4 Calibrated values of controlled ICE power as a function of battery SOC and SOH.

J_{PSO} for the baseline (non-SOH adaptive) EMS is similar to the one illustrated in (2). Nevertheless, a single value of battery SOH (SOH_i) is considered in this case (i.e. $N=1$) corresponding to 0.95.

The PSO toolbox made available in Matlab® software by the Yarpiz project has been used in this work [15]. The swarm size is set to 200 particles, while 100 iterations of the algorithm are performed. Here, the battery SOC is set to 60% of the available capacity at the beginning of each simulation. Values for the inertia coefficient, the cognitive coefficient and the social coefficient are set to 0.73, 1.5 and 1.5, respectively. Fig. 4 illustrates the calibrated values for the controlled ICE power as a function of both SOC and SOH. The SOH adaptive EMS thus selects the instantaneous value of controlled ICE power by interpolating in a two-dimensional lookup table with battery SOC and battery SOH as independent variables. It should be noted that the baseline HEV EMS only uses the calibrated curve for SOH=0.95 in Fig. 4 throughout the vehicle life.

IV. RESULTS

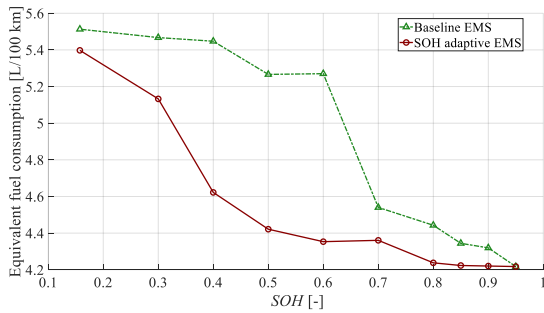
In this section, the fuel economy achieved for the baseline and SOH adaptive HEV EMSs is presented for ten different values of battery SOH. Fig. 5 shows the results both in terms of equivalent fuel consumption as a function of battery SOH and of equivalent fuel consumption increase compared with new battery conditions for both the baseline and battery SOH adaptive EMS.

Results show that the proposed battery SOH adaptive EMS enables the powertrain to only have an increase in fuel consumption of around 4.8% when battery SOH is 0.50, compared to an increase of around 25% for the baseline non-adaptive EMS. Even for a lightly aged battery, the SOH adaptive EMS achieves a few percent better fuel economy than the baseline EMS.

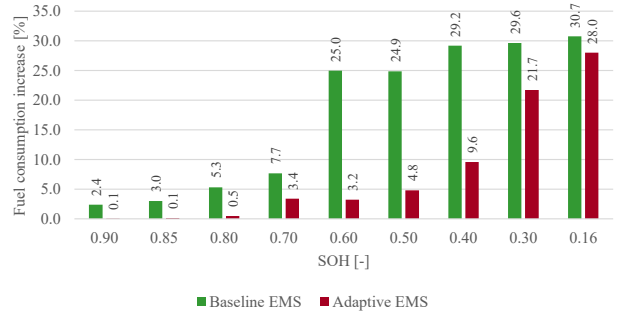
Table II reports simulation statistics for both HEV EMSs considering values of battery SOH equal to 0.80, 0.50 and 0.16, respectively. Time series of battery SOC and fuel rate in WLTP for the three selected values of battery SOH are illustrated in Fig. 6 for both the SOH adaptive EMS and the baseline non-adaptive EMS. Finally, Fig. 7 shows a graphical representation of the contribution of each HEV powertrain loss term in the entire WLTP for the three selected values of SOH. EM instantaneous losses can be evaluated by interpolating in

TABLE II
SIMULATION STATISTICS FOR THE BASELINE HEV EMS AND THE SOH ADAPTIVE HEV EMS CONSIDERING DIFFERENT VALUES OF BATTERY SOH

		SOH = 0.80		SOH = 0.50		SOH = 0.16	
		Baseline EMS	SOH adaptive EMS	Baseline EMS	SOH adaptive EMS	Baseline EMS	SOH adaptive EMS
Energy loss [kJ]	EM1 loss	280	235	467	281	459	447
	EM2 loss	1141	1156	823	1090	618	775
	Transmission loss	1445	1397	2001	1459	2069	2059
	Friction brake loss	151	130	1583	481	2530	1845
	Battery loss	1041	1050	585	1096	167	589
Simulation statistics	ICE off time [%]	64	71	24	64	15	16
	ICE mechanical energy [Wh]	3386	3195	3797	3291	3806	3725
	ICE average efficiency $\bar{\eta}_{ICE}$ [%]	36.9	37.3	35.0	37.1	33.6	33.9
	Fuel consumption [grams]	772	721	915	747	954	927
	Net battery energy variation E_{batt} [Wh]	-112	54	-119	80	-11	29



(a) WLTP equivalent fuel consumption



(b) Equivalent fuel consumption increase compared with new battery conditions (SOH = 0.95)

Fig. 5 Simulation results for the WLTP equivalent fuel consumption as battery ages for the baseline HEV EMS and the SOH adaptive HEV EMS.

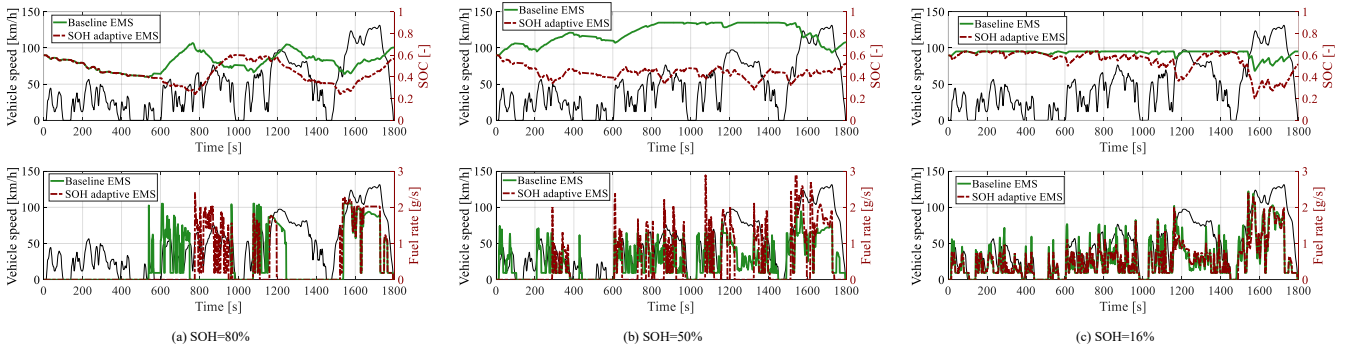


Fig. 6 Time series of battery SOC and fuel rate in WLTP predicted for the baseline HEV EMS and the SOH adaptive HEV EMS considering different values of battery SOH.

the corresponding empirical maps with speed and torque as independent variables. Transmission instantaneous loss is evaluated by considering P_{wheels} and weighting for the two transmission efficiency values reported in Table I for pure electric (EV) and hybrid electric (HEV) operation, respectively. On its behalf, battery pack instantaneous loss is evaluated by multiplying its internal resistance by the squared value of its current.

For lightly aged battery conditions (i.e. SOH=0.80), loss contributions related to EMS, transmission, friction brake and battery exhibit comparable values between baseline non-adaptive and SOH adaptive EMSs in Table II and in Fig. 7. In this case, the SOH adaptive EMS can save fuel mainly by reducing the overall ICE on time (and in turn the transmission loss) and by having the ICE operating in more efficient regions. On the other hand, several contributions can be identified for the fuel economy enhancement of the SOH

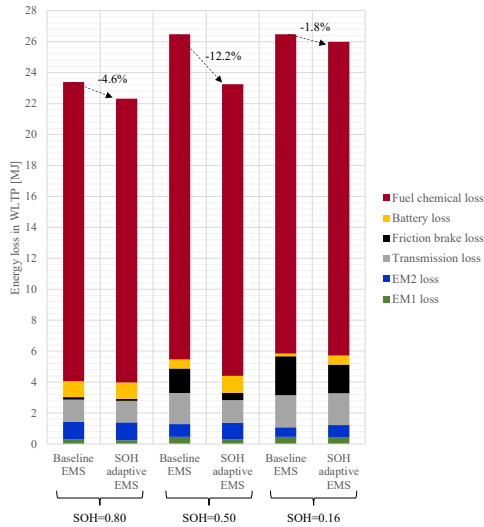


Fig. 7 Energy loss in WLTP predicted for the baseline HEV EMS and the SOH adaptive HEV EMS considering different values of battery SOH.

adaptive EMS when the battery SOH equals 0.50. First, the ICE on time is significantly reduced compared with the baseline non-adaptive EMS, which entails more than 500kJ transmission loss reduction. Second, friction brake loss remarkably decreases by more than 1MJ. Looking at Fig. 6(b), the battery SOC for the baseline non-adaptive EMS constantly exhibits high values (e.g. higher than 70%). Friction brakes need to frequently operate in this case given the limited charge power capability of the battery cells at high SOC [7]. On its behalf, the higher regenerative braking operation of the SOH adaptive EMS reflects in higher losses for both EM2 and battery compared with the baseline non-adaptive EMS. Finally, the battery SOH adaptive EMS enables the ICE average efficiency to increase by more than 2% in this case.

As concerns heavily aged battery conditions (i.e. SOH=0.16), the limited capacity and power capability of the battery pack slightly restrains the potential of the SOH adaptive EMS concerning fuel saving. In particular, it should be noted that in this case the limited pack power capabilities limit the control choices operable by the SOH adaptive EMS. This often prevents the ICE to run at the mechanical power value set by the controller in Fig. 4, yet its power is adjusted to comply with battery operational limits. Nevertheless, the proposed SOH adaptive EMS may still lead to 2% fuel economy improvement and 1.8% energy loss reduction as shown in Fig. 5 and in Fig. 7, respectively. Looking at Fig. 6(c), this can be achieved by the SOH adaptive EMS through allowing the value of battery SOC to broaden throughout the drive cycle compared with baseline non-adaptive EMS. The overall ICE efficiency and the regenerative braking energy capability can be improved in this way.

V. CONCLUSIONS

The worsening of battery performance due to ageing can cause significantly increased fuel consumption for HEVs. To address this issue, this paper proposes a battery SOH adaptive

heuristic EMS that reduces the increase in HEV fuel consumption as the battery ages. PSO is used to optimally calibrate the parameters of the HEV EMS for various levels of battery SOH. The performance of the battery SOH adaptive EMS is benchmarked against a baseline non adaptive EMS which has fixed parameters as the battery ages. The proposed battery SOH adaptive HEV EMS is demonstrated to significantly outperform the baseline controller, reducing fuel consumption as much as 17.4% throughout the lifetime of the battery. Related future work could include the hardware-in-the-loop validation of the proposed EMS, and the investigation of further refined battery SOH adaptive EMS approaches.

REFERENCES

- [1] B. Bilgin et al., "Making the case for electrified transportation," in *IEEE Transactions on Transportation Electrification*, vol. 1, no. 1, pp. 4-17, 2015.
- [2] A. Emadi, "Transportation 2.0: electrified-enabling cleaner, greener, and more affordable domestic electricity to replace petroleum," *IEEE Power Energy Mag.*, vol. 9, no. 4, pp. 18-29, Jul./Aug. 2011.
- [3] R. Xiong, Y. Pan, W. Shen, H. Li, and F. Sun, "Lithium-ion battery ageing mechanisms and diagnosis method for automotive applications: recent advances and perspectives," *Renewable and Sustainable Energy Reviews*, vol. 131, no. 110480, pp. 1-14, 2020.
- [4] "Battery test manual for plug-in hybrid electric vehicles," U.S. Department of Energy, Idaho National Laboratory, Idaho Falls, Idaho 83415, March 2008.
- [5] F. Herb, P. R. Akula, K. Trivedi, L. Jandhyala, A. Narayana, and M. Wöhr, "Theoretical analysis of energy management strategies for fuel cell electric vehicle with respect to fuel cell and battery ageing," *2013 World Electric Vehicle Symposium and Exhibition (EVS27)*, Barcelona, 2013, pp. 1-9.
- [6] S. Saxena, C. Le Floch, J. MacDonald, and S. Moura, "Quantifying EV battery end-of-life through analysis of travel needs with vehicle powertrain models," *J. Power Sources*, vol. 282, pp.265-276, 2015.
- [7] P. G. Anselma et al., "Assessing impact of heavily aged batteries on hybrid electric vehicle fuel economy and drivability," *2021 IEEE Transportation Electrification Conference & Expo (ITEC)*, 2021, pp. 696-70.
- [8] S. Lee, B. Lee, J. McDonald, L. Sanchez, et al., "Modeling and validation of power-split and P2 parallel hybrid electric vehicles," *SAE Technical Paper* 2013-01-1470, 2013.
- [9] P. G. Anselma, P. Kollmeyer, G. Belingardi, and A. Emadi, "Multi-Objective hybrid electric vehicle control for maximizing fuel economy and battery lifetime," *2020 IEEE Transportation Electrification Conference & Expo (ITEC)*, 2020, pp. 1-6.
- [10] P. G. Anselma, P. Kollmeyer, J. Lempert, Z. Zhao, G. Belingardi, and A. Emadi, "Battery state-of-health sensitive energy management of hybrid electric vehicles: lifetime prediction and ageing experimental validation," *Applied Energy*, vol. 281, no. 116440, 2021.
- [11] N. Kim, A. Rousseau, and E. Rask, "Vehicle-level control analysis of 2010 Toyota Prius based on test data," *Proceedings of the Institution of Mechanical Engineers, Part D: Journal of Automobile Engineering*, vol. 226, no. 11, pp. 1483-1494, 2012.
- [12] H. Badshah, D. Kittelson, and W. Northrop, "Particle emissions from light-duty vehicles during cold-cold start," *SAE Int. J. Engines*, vol. 9, no. 3, pp. 1775-1785, 2016.
- [13] A. G. Garcia, L. A. R. Tria, and M. C. R. Talampas, "Development of an energy-efficient routing algorithm for electric vehicles," *2019 IEEE Transportation Electrification Conference and Expo (ITEC)*, 2019, pp. 1-5.
- [14] Hybrid-EV Committee, "Recommended practice for measuring the exhaust emissions and fuel economy of hybrid-electric vehicles, including plug-in hybrid vehicles," *SAE Std. J1711*, Detroit, MI, USA (pp. 13-15), 2010.
- [15] Yarpiz, "Particle swarm optimization in MATLAB," Available online: <https://yarpiz.com/50/ypea102-particle-swarm-optimization> (accessed on 13 April 2022).